Photocatalytic Degradation of Rhodamine B over Sulfated SiO_2-TiO_2 Composite by Sulphuric Acid Impregnation Method

Xue-Min Yan*, Ping Mei, Lin Gao

College of Chemistry and Environmental Engineering, Yangtze University, Jingzhou 434023, PR China

Abstract:

Sulfate modified SiO_2-TiO_2 photocatalysts with different SO_4^{2-} loadings were prepared by incipient-wetness impregnation method using H_2SO_4 solution with various concentrations. The as-prepared SO_4^{2-}/SiO_2-TiO_2 samples were characterized with X-ray diffraction (XRD), scanning electron microscopy (SEM), Brunauer–Emmett–Teller (BET) method, Uv-vis diffuse reflectance spectroscopy (DRS), X-ray photoelectron spectroscopy (XPS) and terephthalic acid photoluminescence probing technique (TA-PL), respectively. The photocatalytic activity of the as-prepared samples was evaluated by photocatalytic degradation of rhodamine B under ultraviolet light irradiation. The effects of H_2SO_4 solution concentration on the structure, morphology, surface properties and photocatalytic activity of SO_4^{2-}/SiO_2-TiO_2 samples were investigated. The results indicated that the catalyst prepared with 4 mol/L H_2SO_4 solution, it showed the highest photocatalytic activity. The higher photocatalytic activity could be attributed to the improved surface properties and the enhanced separation rate of photoinduced electron-hole pairs.

Keywords: Sulfate modification; Photocatalytic activity; Hydroxyl radicals; Surface properties; Rhodamine B

Introduction

Efficient photocatalytic processes have the potential to yield major steps forward in meeting clean energy demand and tackling environmental pollution (1). Titania is the most investigated semiconductor photocatalyst in solar energy conversion and environmental applications because of its low toxicity, low cost, abundance, high photostability, chemical resistance and high efficiency (2-4). V. Murugesan et al. (5, 6) has confirmed that titania can efficiently degrade the different dyes not only under UV irradiation but also under solar light irradiation. The basic principle of semiconductor photocatalysts involves photogenerated electrons and holes migrating to the surface and serving as redox sources that react with adsorbed pollutants, leading to the destruction of pollutants. However, the high rate of recombination of photon-induced electron-hole pairs limits the practical application of TiO_2 materials. Therefore, the improvement and optimization of TiO_2 as photocatalyst is an important task for technical applications of heterogeneous photocatalysis in the future. Many efforts have been performed for the purpose of higher photocatalytic activity of TiO_2 (7-10). The activity of TiO_2 powder depends on its bulk and surface properties (11). It has been noted that porosity of the photocatalyst is quite important for increasing the catalytic performance of the material. However, the titania based materials are usually calcinated above 500 °C for the phase conversion from anatase to rutile, which leads a loss of surface area due to the grain growth (12). Hence, the TiO_2 photocatalyst retains very low specific surface area after calcination, greatly reducing their light-harvesting capability. To enlarge the surface area of TiO_2 and preserve the anatase phase at high calcination temperature, Si-introduced is one of efficient methods. The introduced Si atom inserts into the bulk of the titania, enlarging the surface area, and replace some of Ti^{4+} which resulting in unbalanced positive charges. This causes the SiO_2-TiO_2 composite to adsorb more hydroxyl groups on the particle surface, which is beneficial for photocatalytic reaction (13). Regarding to the surface properties, modification of the titania with different anions such as SO_4^{2-}, PO_4^{3-}, and WO_4^{2-} has been found to enhance the acidity and certain other physico-chemical properties of the catalyst (14-16). In particular, sulfation of semiconductor photocatalysts is of great interest for scientists because it has an enormous potential for environmental pollutant remediation (17, 18). SO_4^{2-}/TiO_2 has been studied by many groups (14, 17-20). Mixed zirconium and titanium sulphated oxides are reported as potential catalysts for the free fatty acids esterification reaction (21). The results demonstrated that the acidity and the surface area of catalysts play an important role in their

*Corresponding author; E-mail: yanzhangmm2002@163.com

 ISSN 1203-8407

catalytic performance. Fu. et al. (20) has attributed the enhanced photocatalytic activity to the improved surface acidities, namely the Lewis acidic sites could react with H_2O and were then converted to Bronsted acidic sites, leading to the activation of water. On the basis of the above analyses, it is considered that sulfated Si-doped TiO_2 may possess high photocatalytic activity.

In the present work, we synthesized sulfate modified SiO_2-TiO_2 photocatalysts by incipient-wetness impregnation method using H_2SO_4 solution with various concentrations. The bulk and surface properties of these SO_4^{2-}/SiO_2-TiO_2 photocatalysts were investigated. The effects of the formation rate of hydroxyl radicals on the photocatalytic activity of SO_4^{2-}/SiO2-TiO_2 photocatalysts have also been carried out.

Methods and Experiment

Synthesis of Photocatalyst

All the reagents (analytical grade) purchased from the Chinese medicine group chemical reagent co. were used as received, LTD. SiO_2-TiO_2 containing 16.6 mol% SiO_2 was fabricated according to the procedure given in reference (22). SO_4^{2-}/SiO_2-TiO_2 photocatalysts with different SO_4^{2-} loadings were prepared by incipient-wetness impregnation method using H_2SO_4 solution with various concentrations. In a typical synthesis, a certain concentration of H_2SO_4 solution was added into a clear beaker and the volume of H_2SO_4 solution is the water pore volume of 4.0 g SiO_2-TiO_2, then 4.0 g SiO_2-TiO_2 was added into the H_2SO_4 solution mentioned above and ultrasonic dispersed for 30 min. After that, the mixture was kept in a static condition for 1h, dried in 353 K for 1h, and then dried in 373 K overnight. Finally, the samples were heated in air at 573K for 2h. The sulfate modified samples with different mol concentration of H_2SO_4 (0 mol/L, 0.5 mol/L, 1 mol/L, 3 mol/L, 4 mol/L and 5 mol/L) were obtained.

Characterization of the Photocatalyst

X-ray diffraction (XRD) patterns were recorded on a Rigaku D/MAX-RB diffractometer with a Cu Ka radiation operating at 40 kV, 50 mA. The specific surface area and pore size measurements were performed on an SSA-4200 automatic surface analyzer (Builder, China). Scanning electron microscope (SEM) images were taken with a JSM-5610 scanning electron microscope (JEOL, Japan), using an accelerating voltage of 20 kV. Diffuse reflectance UV–vis spectra were measured with a spectrometer of PE Lambda 35 equipped with the integrating sphere using $BaSO_4$ as the reference. X-ray photoelectron spectroscopy (XPS) data were collected using a Kratos XSAM800 spectrometer. Fourier-transform infrared (FT-IR) was characterized using an FT-IR spectrophotometer (NICOLET 6700, America) in KBr pellet. Sulphates amount of samples were determined by ion chromatography (PIC-10). The solutions injected in the ion chromatograph and containing the sulphates were obtained suspending the catalysts in a NaOH solution 0.1 M at ambient temperature and then filtering the liquid through a 0.45μm PTFE filter (20).

The formation of hydroxyl radical (•OH) on the surfave of photoirradiated samples is detected by photoluminescence (PL) technique using terephthalic acid (TA) as a probe molecule. Terephthalic acid readily reacts with •OH to produce highly fluorescent product, 2-hydroxyterephthalic acid. This technique has been widely used in the detection of •OH generated in water (19). 50 mg of photocatalyst was suspended in 50 mL of an aqueous solution containing 20 mM NaOH and 6 mM terephthalic acid (TA). The solution was stirred in the dark for 40 min before exposure to UV light. After illumination with a 500 W high-pressure mercury lamp for 20 min, the supernatant was sampled for analysis by recording the fluorescence signal of the generated 2-hydroxyterephthalic acid (TAOH) on a fluorescence spectrometer (Cary Eclips, Agilent, USA). The wavelength of the excitation light was 312 nm, and the scanning speed was 600 nm·min^{-1}. The widths of the excitation slit and the emission slit were both 5 nm. For sulfated photocatalyst, the pH was adjusted by sodium hydroxide solution.

Photocatalytic Degradation Procedure

The as-prepared materials were employed as photocatalysts in the degradation aqueous rhodamine B. The photocatalytic activities were performed at 25 ºC with exterior irradiation. The irradiation source was a 500 W high-pressure mercury lamp with a maximum emitting radiation of 365 nm. In the typical run, 100 mg of photocatalyst was dispersed in 125 mL of rhodamine B (10 mg/L initial concentration), and the pH value of rhodamine B solution was 7.0. The reactor with a double layer cooled by running water to keep the temperature unchanged. The samples were maintained in the dark for 30 mins in order to complete adsorption at equilibrium prior the irradiation. Then, the suspension was illuminated by the high-pressure mercury lamp with magnetic stirring. At given time intervals, about 4 mL aliquots were sampled, centrifuged, and analyzed using an UV-spectrophotometer Perkin Elmer, Lambda 35 at λ_{max} of 553 nm. The rhodamine B concentrations were estimated using a

standard calibration curve. The decolorization efficiency was determined by the formula: decolorization = $(C_0 - C)/C_0$, where C_0 and C represent the initial and residual concentrations, respectively, of rhodamine B dye. The total organic carbon (TOC) content of rhodamine B aqueous was detected by TOC analyser (TOC-3000).

Results and Discussion

Crystal Structure, Morphology and Porosity

Figure 1 showed XRD patterns of SO_4^{2-}/SiO_2-TiO_2 samples prepared with different concentration of H_2SO_4 solution. It can be seen that the diffraction peaks of all samples were indexed with the anatase phase of TiO_2. No new phase is detected in SiO_2-TiO_2 samples after modification by H_2SO_4 solution. It indicates that the crystalline structures of SiO_2-TiO_2 samples have not changed in the process of H_2SO_4 modification and sulfate are only loaded on the surface of SiO_2-TiO_2 samples. The results of ion chromatography indicate that the sample calcined at 573K slightly loses part of its surface sulphates groups. The SO_4^{2-} loadings of various samples are 1.0 wt%, 2.1 wt%, 6.3 wt%, 8.3wt%, and 10.2wt%, and named with SO_4^{2-}/SiO_2-TiO_2(0%), SO_4^{2-}/SiO_2-TiO_2(1.0%), SO_4^{2-}/SiO_2-TiO_2(2.1%), SO_4^{2-}/SiO_2-TiO_2 (6.3%), SO_4^{2-}/SiO_2-TiO_2(8.3%) and SO_4^{2-}/SiO_2-TiO_2(10.2%), respectively.

The morphology of the prepared samples was investigated via SEM experimental analysis. Figure 2 shows SEM pictures of two representative catalysts (0% and 8.3%). As shown in Figure 2, the two catalysts have irregular agglomerated powder morphology. There are not obviously differences in morphology for these two catalysts. However, the size of agglomerate after modified by H_2SO_4 solution has increased, which is harmful to obtain a high-surface-area catalyst. It indicates that the process of sulfate modification can aggravate the agglomeration of catalyst particles. Table 1 lists the specific surface area of various catalysts. SiO_2-TiO_2 sample without sulfate modification have higher specific surface area than SO_4^{2-}/SiO_2-TiO_2 samples. It is consistent with the SEM experiment. With the increase of H_2SO_4 solution concentration, the specific surface area and pore volume of SO_4^{2-}/SiO_2-TiO_2 catalysts decrease. The results are the same as that reported by Zhong (19). TiO_2 surface is positively charged in acidic media. In the H_2SO_4 solution, electrostatic interactions between the positive SiO_2-TiO_2 surface and SO_4^{2-} lead to strong adsorption of the latter on the oxide support. The higher sulphate loading may plugged more pores and resulted in a reduction of total pore volume to some extent and also decrease in surface area. Samantaray et al. (20) reported that the surface area increases (from 64 to 102m^2/g) with an increase in sulfate loading to7.5wt%. They indicated that the Ti–O–Ti bond strength changed in the calcination process, which leads to the formation of porous network. The different results in BET surface area may be due to the different precursor of SO_4^{2-} and post-treatment temperatures, and more detailed mechanism needs to be further investigated in the near future. Generally, the heterogeneous photocatalysis is a surface-based process, and therefore a larger surface area provides more surface active sites for the adsorption of reactant molecules, which thus make the photocatalytic process more efficient (23, 24).

Table 1. The specific surface parameter of various photocatalysts.

Photocatalyst (SO_4^{2-} wt%)	S_{BET}(m^2/g)	Pore volume (cc/g)	Pore size(Å)
0	179	0.093	10.1
1.0	136	0.085	10.2
2.1	122	0.071	10.2
6.3	108	0.069	10.3
8.3	94	0.054	10.7
10.2	93	0.051	10.8

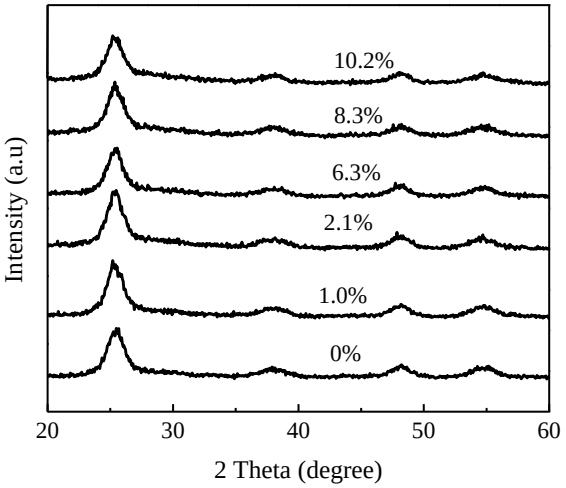

Figure 1. The XRD patterns of different samples.

Surface Sulfur Species

The structure of sulfur complexes on the surface of SiO_2-TiO_2 was examined by XPS and IR measurements. Figure 3A shows the XPS spectrum in the S_{2p} binding energy (BE) region for sulfated SiO_2-TiO_2 samples. The BE of 168.6 eV has been observed, which suggests that the sulfur in SO_4^{2-}/SiO_2-TiO_2 catalysts existed in a six-oxidation state (S^{6+}) (25). Accordingly, it demonstrates that the SO_4^{2-} loaded in the surface of catalysts without the change of structure.

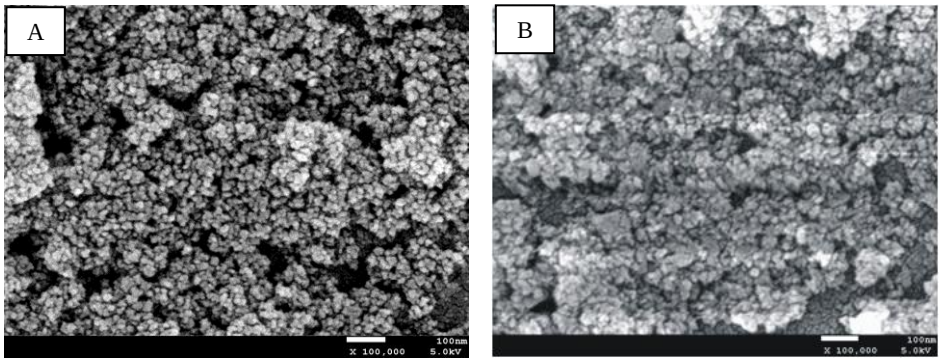

Figure 2. SEM images of photocatalysts: (A) SiO_2-TiO_2 (0%) and (B) SO_4^{2-}/SiO_2-TiO_2 (8.3%).

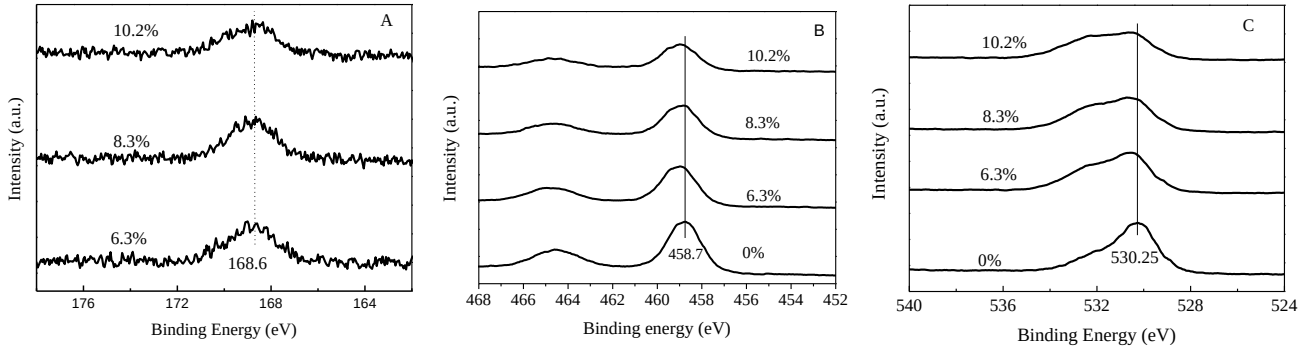

Figure 3. XPS spectra of various samples in (A) S 2p, (B) Ti 2P, and (C) O 1s binding energy regions.

Figure 4 shows the IR spectra of various samples. Several absorption peaks in the 900-1300cm^{-1} region were observed on the sulfated SiO_2-TiO_2 samples but absent on the one for the pristine SiO_2-TiO_2 catalyst. The peaks at 1225,1140, 1040 and 976 cm^{-1} were the characteristic frequencies of a bidentate SO_4^{2-} co-ordinated to metals such as Ti^{4+} (25). It have been reported (20) that such a bridge bidentate structure could strongly withdraw electrons from the neighboring Ti cations, resulting in an up-shifting of BE of the Ti cations. As shown in Figure 3B, $Ti_{2p3/2}$ BE of 458.7 eV was observed for SiO_2-TiO_2 catalyst, while the Ti2p3/2 BE of SO_4^{2-}/SiO_2-TiO_2 catalysts shift to a higher value of 459.9eV, indicating a strong interaction between the sulfate anion and titanium cation. The interaction is usually considered as a driving force in the generation of large amount of surface acidic sites on solid acids of sulfated metal oxides (26). The O1s signals of various samples are shown in Figure 3C. There are also an up-shifting of the BE of oxygen for sulfated SiO_2-TiO_2 catalyst. Oxygen with higher BE can serve as an electron trap to inhibit the recombination of photo-induced electrons and holes (27).

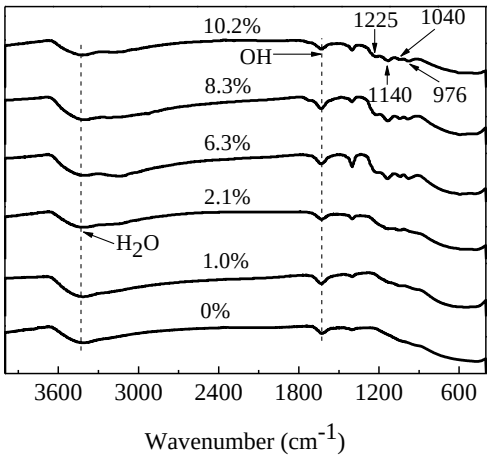

Figure 4. IR spectra of various samples.

Hydroxyl Radical Analysis

Generally, the greater the formation rate of ·OH radicals is, the higher separation efficiency of electron-hole pairs is achieved. In addition, ·OH radical is an extremely strong, nonselective oxidant (E^0 = +3.06 V), which can mineralize the pollutants. So, the photocatalytic activity is in positive correlation to the formation rate of ·OH radicals, namely, a faster formation rate of ·OH radicals leads to a higher photocatalytic activity (28). The PL emission spectra of various samples are shown in Figure 5. It is clear that an obvious PL peak at ca. 425 nm is observed, suggesting that ·OH radicals are formed during the photocatalytic process. It also can be easily seen that the formation rate of ·OH radicals increases with an increase of sulphate loading from 0% to 8.3%, and

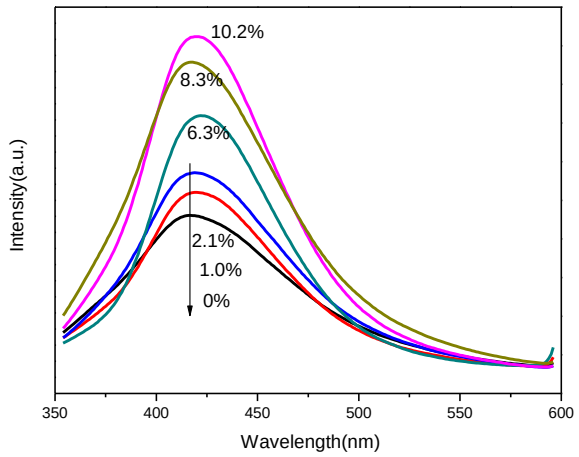

Figure 5. PL spectral changes of different photocatalysts in TA solution.

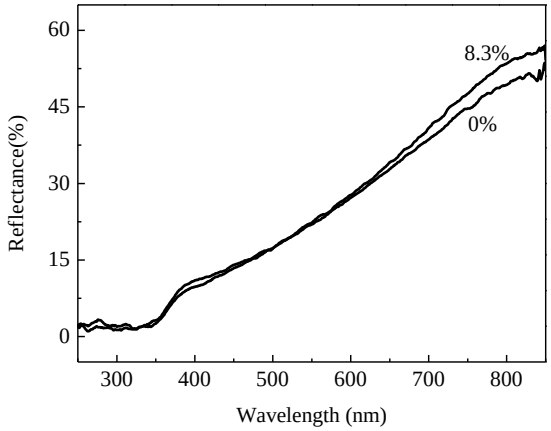

Figure 6. UV-Vis diffuse reflectance spectra of photocatalysts.

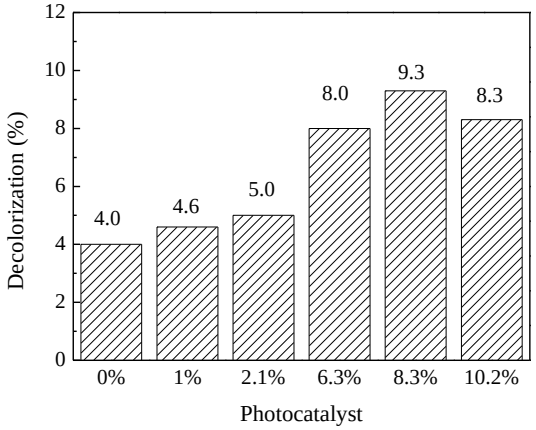

Figure 7. Adsorption of rhodamine B on the different photocatalysts after 30min in dark.

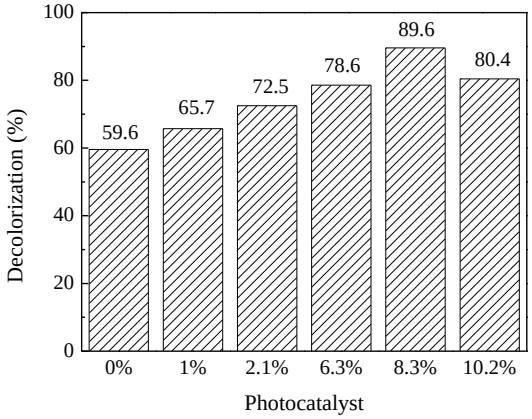

Figure 8. Removal of rhodamine B over various photocatalysts for 3h.

then decreases at even higher sulphate loading. This implies that the sulfated SiO_2-TiO_2 catalysts have higher photocatalytic activity than the pristine SiO_2-TiO_2 catalyst. Further observation shows that the optimum sulphate loading is 8.3%.

Optical Property and Photocatalytic Activity

Figure 6 shows diffuse reflectance spectra of SiO_2-TiO_2 and sulfated SiO_2-TiO_2. Due to the partial overlap of the diffuse reflectance spectra of sulfated SiO_2-TiO_2 samples, only the diffuse reflectance spectra of SiO_2-TiO_2 and SO_4^{2-}/SiO_2-TiO_2 (8.3%) were presented. Compared to SiO_2-TiO_2, it is clear that the presence of SO_4^{2-} have not change the reflectance of photocatalysts in the visible light range. It indicates that sulfate process has not obvious effect on the energy-band structure of SiO_2-TiO_2 catalyst. Accordingly, the improved photocatalytic performance of SO_4^{2-}/SiO_2-TiO_2 might be attributed to the changes of surface properties.

The adsorption of rhodamine B on different photocatalysts after 30 min in dark is shown in Figure 7. The adsorption of rhodamine B tends to increase with the increase of sulphate loading. Among these photocatalysts, 8.3% sulphate loading has the highest adsorption toward rhodamine B. The higher adsorption can be attribute to the formation of the solid super-acid, which will enhance Lewis acidity of metal center ions and promote the acidic sites on the TiO_2 surface. However, a large amount of the SO_4^{2-} is harmful for the adsorption possibly due to the coverage of too many TiO_2 active sites by the SO_4^{2-}. The photocatalytic activities of the obtained SO_4^{2-}/SiO_2-TiO_2 were tested by the degradation of rhodamine B solution under UV light irradiation. The order of photocatalytic activity is SO_4^{2-}/SiO_2-TiO_2 (8.3%) $>$ SO_4^{2-}/SiO_2-TiO_2 (10.2%) $>$ SO_4^{2-}/SiO_2-TiO_2 (6.3%) $>$ SO_4^{2-}/SiO_2-TiO_2 (2.1%) $>$ SO_4^{2-}/SiO_2-TiO_2 (1.0%) $>$ SO_4^{2-}/SiO_2-TiO_2 (0%), all sulfated SiO_2-TiO_2 catalysts exhibit better photocatalytic performance than the pristine SiO_2-TiO_2 catalyst and the SO_4^{2-}/SiO_2-TiO_2 (8.3%) sample possesses the best photocatalytic performance. The complete mineralisation is confirmed from total organic carbon (TOC) content. Figure 8 shows the

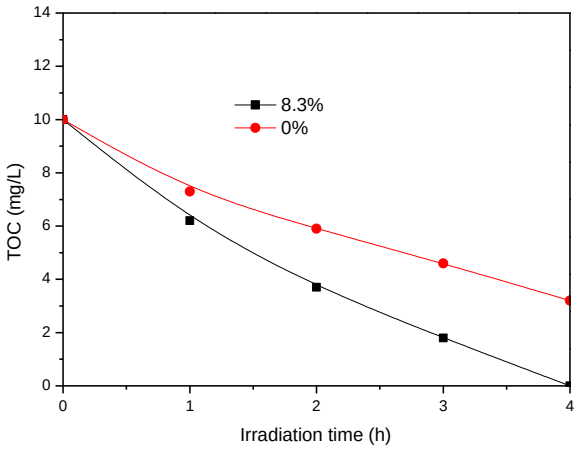

Figure 9. TOC values vs. irradiation time.

degradation of organic carbon content of rhodamine B with SO_4^{2-}/SiO_2-TiO_2 (0%) and SO_4^{2-}/SiO_2-TiO_2 (8.3%) as photocatalyst. TOC values decrease with increase in irradiation time. The rhodamine B can be mineralised into harmless end products after 4 h irradiation with SO_4^{2-}/SiO_2-TiO_2 (8.3%) as photocatalyst. These results suggest that the process of sulfate modification can enhance the photocatalytic activity of SiO_2-TiO_2 and that there is an optimum H_2SO_4 solution concentration for the sulfate modification. The excess SO_4^{2-} make against the photocatalytic activity possibly due to the coverage of active sites by the SO_4^{2-} (27).

It was noted that both bulk properties (e.g. surface area, crystal phase, and crystal size) and surface properties considerably affect the photocatalytic activity of SiO_2-TiO_2 catalysts (29). Among these catalysts, SO_4^{2-}/SiO_2-TiO_2 catalysts possess the slower specific surface area but show the higher photocatalytic activity than SiO_2-TiO_2 catalyst. So, the improved photocatalytic performance of SO_4^{2-}/SiO_2-TiO_2 might be attributed to their surface properties. The sulfation of SiO_2-TiO_2 photocatalyst induced Bronsted acidic sites and increased Lewis acidic sites on the surface of SiO_2-TiO_2 (20). The strong acidities imparted a high reactivity on SiO_2-TiO_2 surface toward adsorbing reactant and oxygen molecules (20).The surface acidic sites on SO_4^{2-}/SiO_2-TiO_2 catalyst can enhanced the adsorption of rhodamine B. When the adsorption of rhodamine B is enhanced, the total degradation process will be greatly accelerated. In addition, the photogenerated electrons can either reduce the dye or can react with surface adsorbed O_2 to create superoxide radicals (O_2^{-}•). Among various primary photocatalytic processes on TiO_2, the interfacial transfer of photoinduced electron is the slowest step, and therefore, it is a rate-determining step (30). The increase in oxygen adsorption is favorable for the interfacial transfer of photoexcited electrons, which will help to accelerate the process of the photocatalytic degradation.

Moreover, the higher photocatalytic activity of SO_4^{2-}/SiO_2-TiO_2 in the degradation of rhodamine B could also be attributed to the higher separation rate of photoinduced charge carriers. During the photocatalytic process, the photogenerated holes can oxidize the organic molecules or react with surface adsorbed water to form hydroxyl radicals (OH•). The hydroxyl radicals can partial or complete oxide the organic pollutants presenting at or near the surface of photocatalyts (31). So, the higher separation rate of photoinduced charge carriers is beneficial to form hydroxyl radical, and then enhance the photocatalytic activity. As shown in the results of hydroxyl radical analysis, the SO_4^{2-}/SiO_2-TiO_2 (8.3%) catalysts possesses the highest formation rate of ·OH radicals, reflecting the highest separation rate of photoinduced electron-hole pairs.

The recycling of the catalyst in the degradation aqueous rhodamine B was also investigated with SO_4^{2-}/SiO_2-TiO_2 (8.3%) as catalyst. After each run, the catalyst was separated by filtration, washed with deionized water, heated at 573 K for 2 h, and then placed into a fresh reagent mixture. The removal of sulfur for the three runs was 89.6, 86.2 and 85.3%, respectively, indicating that the catalyst was stable under operating conditions.

Conclusions

Sulfate modified SiO_2-TiO_2 photocatalysts can be facilely prepared by a simple incipient-wetness impregnation method using H_2SO_4 solution. The formation rates of hydroxyl radicals and photocatalytic degradation of rodamine B aqueous solution were significantly enhanced by sulfate modification on the surface of SiO_2-TiO_2 photocatalyst. The SO_4^{2-}/SiO_2-TiO_2 (8.3%) catalyst showed the best photocatalytic activity for photocatalytic degradation of rodamine B aqueous solution due to the enhanced surface acidities and improved separation rate of photoinduced charge carriers. In addition, the catalyst also shows excellent reusing ability, which makes it a promising catalyst in the degradation aqueous rhodamine B.

Acknowledgements

The authors are grateful for the financial support provided by Chinese National Science Foundation (21106008, 51472034).

References

(1) Leary, R.; Westwood, A. *Carbon* **2011**, *49*, 741-772.

(2) Asahi, R.; Morikawa, T.; Ohwaki, T.; Aoki, K.; Taga, Y. *Science* **2001**, *293*, 269-271.

(3) Khan, S.U.M.; Al-Shahry, M.; Ingler, W.B. *Science* **2002**, *297*, 2243-2245.

(4) Zhao, L.; Chen, X.; Wang, X.; Zhang, Y.; Wei, W.; Sun, Y.; Antonietti, M.; Titirici, M.M. *Adv. Mater*. **2010**, *22*, 3317-3321.

(5) Neppolian, B.; Choi, H.C.; Sakthivel, S.; Arabindoo, B.; Murugesan, V. *Journal of Hazardous Materials B* **2002**, *89*, 303-317.

(6) Neppolian, B.; Choi, H.C.; Sakthivel, S.; Arabindoo, B.; Murugesan, V. *Chemosphere* **2002**, *46*, 1173-1181.

(7) Burda, C.; Lu, Y.; Chen, X.; Samia, A.C.S.; Stout, J.; Gole, J.L. *Nano Lett*. **2003**, *3*, 1049-1051.

(8) Yu, J.C.; Ho, W.; Yu, J.; Yip, H.; Wong, P.K.; Zhao, J. *Environ. Sci. Technol*. **2005**, *39*, 1175-1179.

(9) Wang, X.H.; Li, J.G.; Kamiyama, H.; Moriyoshi, Y.; Ishigaki, T. *J. Phys. Chem. B* **2006**, *110*, 6804-6809.

(10) Li, H.; Bian, Z.; Zhu, J.; Hu, Y.; Li, H.; Lu, Y. *J. Am. Chem. Soc*. **2007**, *129*, 4538-4539.

(11) Lisenbigler, A.; Lu, G.; Yates, J. *Chem. Rev*. **1995**, *95*, 735-758.

(12) Chen, Q.; Shi, H.; Shi, W.; Xu, Y.; Wu, D. *Catal. Sci. Technol*. **2012**, *2*, 1213-1220.

(13) Hou, Y.D.; Wang, X.C.; Wu, L.; Chen, X.F.; Ding, Z.X.; Wang, X.X.; Fu, X.Z. *Chemosphere* **2008**, *72*, 414-421.

(14) Dalai, A.K.; Sethuraman, R.; Katikaneni, S.P.R.; Idem, R.O. *Ind. Eng. Chem. Res*. **1998**, *37*, 3869-3878.

(15) Samantaray, S.K.; Parida, K.M. *Appl. Catal. A*. **2001**, *220*, 9-20.

(16) Reddy, B.M.; Sreekanth, P.M.; Yamada, Y.; Xu, Q.; Kobayashi, T. *Appl. Catal. A* **2002**, *228*, 269-278.

(17) Parida, K.M.; Sahu, N.; Biswal, N.R.; Naik, B.; Pradhan, A.C. *J. Coll. Interf. Sci*. **2008**, *318*, 2231-237.

(18) Xie, C.; Yang, Q.; Xu, Z.; Liu, X.; Du, Y. *J. Phys. Chem. B*, **2006**, *110*, 8587-8592.

(19) Zhong, J.; Li, J.; Zeng, J.; Huang, S.; Hu, W.; Chen, J.; Li, M.; Wang, J.; Zhang, S. *Mater. Sci. Semicond. Process*. **2014**, *26*, 62-68.

(20) Wang, X.; Yu, J.C.; Liu, P.; Wang, X.; Su, W.; Fu, X. *J. Photochem. Photobiol. A* **2006**, *179*, 339-347.

(21) Boffito, D.C.; Crocellà, V.; Pirola, C.; Neppolian, B.; Cerrato, G.; Ashokkumar, M.; Bianchi, C.L. *Journal of Catalysis* **2013**, *297*, 17-26.

(22) Mohamed, R.M. *J. Mater. Process. Tech*. **2009**, *209*, 577-583.

(23) Samantaray, S.K.; Mohapatra P.; Parida, K. *J. Mol. Catal. A: Chem.* **2003**, *198*, 277-287.

(24) Zhou, M.; Zhang, J.; Cheng, B.; Yu, H. *Int. J. Photoenergy* **2012**, *532843*, 1-10.

(25) Sohn, J.R.; Jang, H.J.; Park, M.Y.; Park, E.H.; Park, S.E. *J. Mol. Catal*. **1994**, *93*, 149-167.

(26) Sohn, J.R.; Kim, H.J. *J. Catal*. **1986**, *101*, 428-433.

(27) Li, H.; Li, G.; Zhu, J.; Wan, Y. *J. Mol. Catal. A: Chem*. **2005**, *226*, 93-100.

(28) Yu, J.; Xiang, Q.; Zhou, M. *Appl. Catal. B* **2009**, *90*, 595-602.

(29) Colóna, G.; Hidalgoa, M.C.; Munueraa, G.; Ferinob, I.; Cutrufellob, M.G.; Navíoa, J.A. *Appl. Catal. B* **2006**, *63*, 45-59.

(30) Hoffmann, M.R.; Martin, S.T.; Choi, W.; Bahnemann, D.W. *Chem. Rev*. **1995**, *95*, 69-96.

(31) Fouad, O.A.; Ismail, A.A.; Zaki, Z.I.; Mohamed, R.M. *Appl. Catal. B* **2006**, *62*, 144-149.

Received for review August 19, 2014. Revised manuscript received July 10, 2015. Accepted September 16, 2015.